

Planar three-loop QCD helicity amplitudes for V +jet production at hadron colliders

Thomas Gehrmann^a, Petr Jakubčík^a, Cesare Carlo Mella^b, Nikolaos Syrrakos^b, Lorenzo Tancredi^b

^aPhysik-Institut, Universität Zürich, Winterthurerstrasse 190, CH-8057 Zürich, Switzerland

^bTechnical University of Munich, TUM School of Natural Sciences, Physics Department, James-Frank-Straße 1, 85748 Garching, Germany

Abstract

We compute the planar three-loop Quantum Chromodynamics (QCD) corrections to the helicity amplitudes involving a vector boson $V = Z, W^\pm, \gamma^*$, two quarks and a gluon. These amplitudes are relevant to vector-boson-plus-jet production at hadron colliders and other precision QCD observables. The planar corrections encompass the leading colour factors N^3 , N^2N_f , NN_f^2 and N_f^3 . We provide the finite remainders of the independent helicity amplitudes in terms of multiple polylogarithms, continued to all kinematic regions and in a form which is compact and lends itself to efficient numerical evaluation. The presented amplitude respects the conjectured symbol-adjacency constraints for amplitudes with three massless and one massive leg.

1. Introduction

Scattering amplitudes provide the connection between the Lagrangian formulation of the Standard Model of particle physics and observable quantities at particle collider experiments. Their perturbation theory expansion amounts to the computation of loop corrections, enabling increasingly accurate predictions. Multi-loop amplitudes in QCD provide moreover an important gateway for new mathematical ideas to enter particle physics.

The helicity amplitudes for processes involving a vector boson and three partons have been of pivotal importance to QCD precision physics. In their different kinematical crossings, these amplitudes describe three-jet production in e^+e^- annihilation [17], (2+1)-jet production in deep inelastic ep scattering, and V +jet production at hadron colliders. Measurements of all three types of processes allowed establishing QCD as the correct theory of the strong interactions. Precision data on these benchmark reactions continue to play a key role in enabling accurate determinations of the QCD coupling constant and of the partonic content of the proton.

On the theoretical side, these processes are also a testing ground for the development of new calculational methods in perturbative QCD. $e^+e^- \rightarrow 3$ jets was the first jet production process to be computed to next-to-leading order (NLO, [18]) and next-to-next-to-leading order (NNLO, [28, 52]), thereby driving the development of systematic formulations of both subtraction and phase-space slicing methods for handling infrared singularities and their implementation in flexible parton-level event generation programs [11, 29, 31, 39]. It is likely that $e^+e^- \rightarrow 3$ jets will be among the first processes with jets to be tackled at third order (N^3 LO) in perturbative QCD.

At the LHC, leptonic decays of produced vector bosons leave clear signatures in the detectors, allowing observables such as the transverse momentum distribution of the lepton pair to be measured to a precision well below the percent level. To match this level of accuracy requires going beyond the currently avail-

able NNLO predictions [4, 30, 43] for vector-boson-plus-jet production, which relates directly to the vector boson transverse momentum spectrum.

The Born-level helicity amplitudes for these processes couple the vector boson to a quark-antiquark pair and a gluon: $Vq\bar{q}g$. QCD corrections to these amplitudes were computed previously up to one loop [31] and two loops [20], recently extended to include singlet axial vector coupling terms [23] and higher orders in the dimensional regulator [22].

The extension of scattering amplitudes to the next loop order is always associated with conceptual advances. More than twenty years ago, the calculation of the two-loop master integrals for four-point functions with one off-shell leg [25, 26] served as the first advanced example of the use of the method of differential equations [24, 38], now ubiquitous in multi-loop calculations. It also necessitated the study of a new class of functions, generalized harmonic polylogarithms (multiple polylogarithms, MPLs) [26, 32].

The concept of a canonical basis of master integrals [2, 35] has facilitated the extension of the two-loop $Vq\bar{q}g$ master integrals to transcendental weight six [21]. At three loops, the ladder-box topology was considered some time ago [13], while the more challenging tennis court topologies have only been addressed more recently [5, 6]. Interestingly, all planar integrals can be expressed in terms of MPLs with the same alphabet as at two loops. On the other hand, the first results for non-planar topologies [6, 33] indicate an extended alphabet with the appearance of square roots. The increasing complexity at intermediate stages of amplitude calculations has also led to the adoption of methods based on finite-field arithmetic in particle physics [42, 45], allowing the reconstruction of analytic results for the amplitudes from multiple numerical evaluations.

This combination of conceptual and technical developments enables us to derive the planar three-loop QCD $Vq\bar{q}g$ helicity amplitudes, which we present in this letter. These amplitudes constitute the virtual N^3 LO QCD corrections to $e^+e^- \rightarrow 3$ jets and processes related to it by kinematical crossing, and are the

stepping stone to reach a new level of precision in QCD studies at colliders.

2. Setup and Calculation

We consider the production of a vector boson V through lepton-antilepton annihilation and its subsequent decay into a quark, anti-quark and a gluon

$$l^+(p_5) + l^-(p_6) \rightarrow V(p_4) \rightarrow q(p_1) + \bar{q}(p_2) + g(p_3). \quad (1)$$

The calculation is performed assuming a purely vector coupling for V and the effect of non-singlet axial couplings is reconstructed later by reweighting the helicity amplitudes by the appropriate couplings, see eq. (14). We introduce the usual Mandelstam invariants

$$s_{12} = (p_1 + p_2)^2, \quad s_{13} = (p_1 + p_3)^2, \quad s_{23} = (p_2 + p_3)^2$$

which satisfy the conservation equation

$$s_{12} + s_{13} + s_{23} = q^2, \quad (2)$$

where $q^2 = p_4^2$ is the momentum-squared of the vector boson. It is convenient to work with the following dimensionless ratios

$$x = s_{12}/q^2, \quad y = s_{13}/q^2, \quad z = s_{23}/q^2, \quad (3)$$

such that (2) implies $x + y + z = 1$. It is easy to see that in the decay kinematic region all these invariants are non-negative and

$$z \geq 0, \quad 0 \leq y \leq 1 - z, \quad x = 1 - y - z. \quad (4)$$

We work in dimensional regularization, taking $d = 4 - 2\epsilon$. In particular, we adopt the 't Hooft-Veltman dimensional regularization scheme [36], in which loop momenta are d -dimensional but external states are kept in four dimensions. The amplitude for the production of a vector boson can then be written as

$$\mathcal{M} = -i\sqrt{4\pi\bar{\alpha}_s} \mathbb{T}_{ij}^a A_{\mu\nu} \epsilon_5^\mu \epsilon_4^\nu, \quad (5)$$

where $\bar{\alpha}_s$ is the bare strong coupling and \mathbb{T}_{ij}^a is the generator of $SU(N)$ in the fundamental representation. We can then proceed by decomposing the amplitude $A^{\mu\nu}$ in eq. (5) into a basis of tensor structures in $d = 4$ spacetime dimensions following a method introduced in [46, 47], see ref. [22] for details.

Instead of calculating the corresponding form factors, we prefer to start from this decomposition and introduce projector operators that directly extract the amplitude for fixed helicities of the external states and contracted with a leptonic current. To this end, we define

$$\mathbb{M}_{\lambda_{q_2}\lambda_3\lambda_5} = \epsilon_{3,\mu}^{\lambda_3} A_{\lambda_{q_1}\lambda_{q_2}}^{\mu\nu} C_{\lambda_5}^\nu(p_5, p_6). \quad (6)$$

Working in spinor-helicity formalism, we write for the left- and right-handed fermionic currents

$$C_L^\mu(p, q) = [q\gamma^\mu p], \quad C_R^\mu(p, q) = [p\gamma^\mu q], \quad (7)$$

and for the polarization vector of the outgoing external gluon

$$\epsilon_{3,-}^\mu = \frac{\langle 3\gamma^\mu 2 \rangle}{\sqrt{2}\langle 32 \rangle}, \quad \epsilon_{3,+}^\mu = \frac{\langle 2\gamma^\mu 3 \rangle}{\sqrt{2}\langle 23 \rangle}, \quad (8)$$

where we adopted an axial gauge with p_2 as the reference vector. In this setup, the two independent helicity amplitudes read

$$\mathbb{M}_{L+L} = \frac{1}{\sqrt{2}} \left[\langle 12 \rangle [13]^2 (\alpha_1 \langle 536 \rangle + \alpha_2 \langle 526 \rangle) + \alpha_3 \langle 25 \rangle [13] [36] \right], \quad (9)$$

$$\mathbb{M}_{L-L} = \frac{1}{\sqrt{2}} \left[\langle 23 \rangle^2 [12] (\gamma_1 \langle 536 \rangle + \gamma_2 \langle 516 \rangle) + \gamma_3 \langle 23 \rangle \langle 35 \rangle [16] \right], \quad (10)$$

and the remaining two helicity amplitudes, \mathbb{M}_{R+L} and \mathbb{M}_{R-L} , can be obtained by means of parity and charge conjugation [22, 23]. Additionally, for each amplitude, the lepton current handedness can be reversed by a simple swap $p_5 \leftrightarrow p_6$. The contribution of a Feynman diagram to the independent helicity coefficients α_i and γ_i with $i = 1, \dots, 3$ can then be obtained by applying suitable projector operators. Their explicit form (immaterial to the present discussion) is given in the supplemental material.

The helicity amplitude coefficients $\Omega = (\alpha_i, \gamma_i)$ can be expanded in powers of the strong coupling constant

$$\Omega = \Omega^{(0)} + \left(\frac{\alpha_s}{2\pi}\right) \Omega^{(1)} + \left(\frac{\alpha_s}{2\pi}\right)^2 \Omega^{(2)} + \left(\frac{\alpha_s}{2\pi}\right)^3 \Omega^{(3)} + \mathcal{O}(\alpha_s^4). \quad (11)$$

This expansion holds for the bare coefficients (with α_s replaced by $\bar{\alpha}_s$), the renormalized coefficients, as well as for the IR-subtracted coefficients defined below. The three-loop coefficients are in turn decomposed into color factors as

$$\begin{aligned} \Omega^{(3)} = & N^3 \Omega_1^{(3)} + N \Omega_2^{(3)} + \frac{1}{N} \Omega_3^{(3)} + \frac{1}{N^3} \Omega_4^{(3)} \\ & + N_f N^2 \Omega_5^{(3)} + N_f \Omega_6^{(3)} + \frac{N_f}{N^2} \Omega_7^{(3)} \\ & + N_f^2 N \Omega_8^{(3)} + \frac{N_f^2}{N} \Omega_9^{(3)} + N_f^3 \Omega_{10}^{(3)} \\ & + N_{f,V} N^2 \Omega_{11}^{(3)} + N_{f,V} \Omega_{12}^{(3)} \\ & + \frac{N_{f,V}}{N^2} \Omega_{13}^{(3)} + N_f N_{f,V} N \Omega_{14}^{(3)} + \frac{N_f N_{f,V}}{N} \Omega_{15}^{(3)}, \end{aligned} \quad (12)$$

where N_f is the number of active quark flavors in the loops, and $N_{f,V}$ denotes contributions where the vector boson couples to an internal fermion loop. In this letter we focus on the dominant terms in this expansion. Using $N_f \sim N$, these are all the terms with total power of three in N and N_f and they correspond to Ω_j with $j = 1, 5, 8, 10$. Importantly, the leading color factors only receive contribution from planar diagrams, see Figure 1 for example diagrams. The contributions proportional to $N_f^2 N_{f,V}$ vanish for a vector-like coupling by Furry's theorem. Eq. (12) is also valid for any helicity amplitude coefficient – bare, renormalized or IR subtracted.

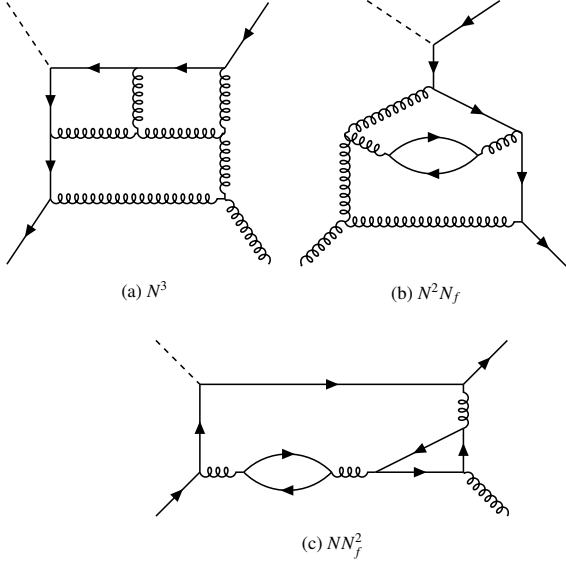


Figure 1: Representative three-loop planar diagrams which contribute to the three leading color layers.

In the following, we fix the renormalization scale in Ω as $\mu^2 = q^2$. The full scale dependence can then be recovered through

$$\begin{aligned} \Omega^{(3)}(\mu) &= \left(\frac{5}{16} \beta_0^3 L(\mu)^3 + \beta_0 \beta_1 L(\mu)^2 + \frac{1}{2} \beta_2 L(\mu) \right) \Omega^{(0)} \\ &+ \left(\frac{15}{8} \beta_0^2 L(\mu)^2 + \frac{3}{2} \beta_1 L(\mu) \right) \Omega^{(1)} \\ &+ \frac{5}{2} \beta_0 L(\mu) \Omega^{(2)} + \Omega^{(3)} \end{aligned} \quad (13)$$

with $L(\mu) = \log(\mu^2/q^2)$.

The helicity amplitudes for the decay of a Standard Model vector boson V can finally be related to the helicity amplitudes obtained above by dressing with the appropriate electroweak couplings

$$\begin{aligned} \mathcal{M}_{\lambda_{q_2}, \lambda_3, \lambda_5}^V &= - \frac{i \sqrt{4\pi\alpha_s} (4\pi\alpha) L_{l_5 l_6}^V L_{q_1 q_2}^V}{D(p_{56}^2, m_V^2)} \\ &\times \mathbb{T}_{ij}^a \mathbf{M}_{\lambda_{q_2}, \lambda_3, \lambda_5}, \end{aligned} \quad (14)$$

where $p_{56} = p_5 + p_6$, the vector boson propagator reads

$$D(q^2, m_V^2) = q^2 - m_V^2 + i\Gamma_V m_V \quad (15)$$

and the couplings for the bosons $V = Z, W^\pm, \gamma^*$ are

$$R_{f_1 f_2}^\gamma = L_{f_1 f_2}^\gamma = -e_{f_1} \delta_{f_1 f_2}, \quad (16)$$

$$L_{f_1 f_2}^Z = \frac{I_3^{f_1} - \sin^2 \theta_w e_{f_1}}{\sin \theta_w \cos \theta_w} \delta_{f_1 f_2}, \quad (17)$$

$$L_{f_1 f_2}^W = \frac{\epsilon_{f_1, f_2}}{\sqrt{2} \sin \theta_w}, \quad (18)$$

$$R_{f_1 f_2}^Z = -\frac{\sin \theta_w e_{f_1}}{\cos \theta_w} \delta_{f_1 f_2}, \quad (19)$$

$$R_{f_1 f_2}^W = 0. \quad (20)$$

In the formulas above, α is the electroweak coupling constant, θ_w is the Weinberg angle, $I_3 = \pm 1/2$ is the third component of the weak isospin and the charges e_i are measured in terms of the fundamental electric charge $e > 0$. Moreover, $\epsilon_{f_1, f_2} = 1$ if $f_1 \neq f_2$ but belonging to the same isospin doublet, and zero otherwise.

In order to compute the (unrenormalized) corrections to the helicity amplitude coefficient, we use the same unified workflow as for the tree-level, one- and two-loop amplitudes for $Vq\bar{q}g$ [22], whose agreement with older results in the literature up to the finite part in ϵ provides an additional check on our method. In summary, the relevant three-loop diagrams are generated using QGRAF [44] and every manipulation including insertion of Feynman rules, evaluation of Dirac and Lorentz algebra and application of the projectors are performed in FORM [50]. Once the helicity projectors have been applied, all Feynman diagrams are expressed in terms of scalar integrals, which can be written in terms of a single planar auxiliary topology of the form

$$\mathcal{I}_{n_1, \dots, n_{15}} = e^{3\gamma_E \epsilon} \int \prod_{i=1}^3 \frac{d^d k_i}{i\pi^{d/2}} \frac{1}{D_1^{n_1} \dots D_{15}^{n_{15}}} \quad (21)$$

with $\gamma_E = 0.5772 \dots$ the Euler constant and propagators

$$\begin{array}{lll} D_1 = k_1 & D_6 = k_3 - p_1 & D_{11} = k_2 - p_{123} \\ D_2 = k_2 & D_7 = k_1 - p_{12} & D_{12} = k_3 - p_{123} \\ D_3 = k_3 & D_8 = k_2 - p_{12} & D_{13} = k_1 - k_2 \\ D_4 = k_1 - p_1 & D_9 = k_3 - p_{12} & D_{14} = k_1 - k_3 \\ D_5 = k_2 - p_1 & D_{10} = k_1 - p_{123} & D_{15} = k_2 - k_3 \end{array}$$

with $p_{ij(k)} = p_i + p_j(+p_k)$. The integrals can be reduced to a set of master integrals using integration-by-parts (IBP) identities [12, 49]. For the actual reduction, we use the implementation of the Laporta algorithm [40] in the automated code KIRA2 [37, 41] and express all integrals directly in terms of the canonical basis for the three-loop planar family defined in [6]. Here it was shown that, in line with the one- and two-loop results, the three-loop planar integrals can be evaluated to arbitrary orders in the dimensional regularization parameter ϵ in terms of multiple polylogarithms (MPLs) [26, 32, 48, 51] with alphabet $\{y, z, 1-y, 1-z, y+z, 1-y-z\}$.

The amplitude before reduction can be expressed in terms of 95625 scalar integrals, which in turn are reduced to 291 canonical basis elements and their crossings. The size and complexity of intermediate expressions makes the use of traditional methods for symbolic insertion of the IBP reduction into the unreduced amplitude highly non-trivial. Therefore, in view of the expected increase in complexity of the subleading layers in the color expansion (12), we also devised a hybrid method involving finite field reconstruction, in parallel to a standard fully analytic approach.

In particular, in the standard approach, we produced the IBP identities with KIRA2 and used MATHEMATICA and FERMAT to include them into the unreduced amplitude and simplify the resulting coefficients. We then expanded the master integrals in ϵ and obtained the final expression for the amplitude in terms

of MPLs. In the hybrid approach, we used the same IBP reduction obtained with KIRA2. However, we then performed an insertion of the reduction and MI solutions in the amplitude for a handful of rational numerical values of the variables y and z in the coefficients of the MPLs. This step allowed us to determine which polylogarithms appear in the final expression for a given helicity coefficient. With this information, we proceeded to reconstruct the rational prefactors in y and z only for the relevant polylogarithms, leveraging the implementation provided by FINTEFLOW [45]. This approach lends itself to parallelization and gives us the possibility to recycle the symbolic reductions in future calculations. Compared to the traditional approach of reconstructing only the finite part, it allows us to present also the renormalized amplitudes with explicit IR poles for greater versatility in phenomenological applications with different pole schemes. We verified that the reconstructed results exactly matched those obtained through the fully analytic approach.

3. UV renormalization and IR subtraction

All UV divergences are removed by expressing the helicity coefficients in terms of the $\overline{\text{MS}}$ -renormalized strong coupling $\alpha_s = \alpha_s(\mu)$. Since this is a standard procedure, we only summarize the necessary β -function coefficients in the supplemental material. The remaining IR divergences are universal and can be extracted multiplicatively in the formalism of Soft-Collinear Effective Theory (SCET) [3, 10, 14, 19] as

$$\mathbf{\Phi}_{\text{finite}}(\{p\}) = \lim_{\epsilon \rightarrow 0} \mathcal{Z}^{-1}(\{p\}; \epsilon) \mathbf{\Phi}(p, \epsilon), \quad (22)$$

where we indicate with $\mathbf{\Phi}_{\text{finite}}(\{p\})$ the finite remainder of the amplitude $\mathbf{\Phi}(p, \epsilon)$. As indicated by the bold font, \mathcal{Z} is generally an operator in color space, but it diagonalizes when acting on the $Vq\bar{q}g$ amplitude coefficients, which factorize onto a single color structure,

$$\mathbf{\Phi} = \mathbb{T}_{ij}^a \Omega. \quad (23)$$

\mathcal{Z} can be formally expressed in terms of the anomalous dimension matrix $\mathbf{\Gamma}$ as

$$\begin{aligned} \mathcal{Z}(\epsilon, \{p\}, \mu) &= \mathbb{P} \exp \left[\int_{\mu}^{\infty} \frac{d\mu'}{\mu'} \mathbf{\Gamma}(\{p\}, \mu') \right] \\ &= \sum_{l=0}^{\infty} \left(\frac{\alpha_s}{2\pi} \right)^l \mathcal{Z}^{(l)}. \end{aligned} \quad (24)$$

Importantly, for the first time at three loops, the anomalous dimension operator is not entirely captured by a dipole term but receives contributions also from quadrupole color correlation operators,

$$\mathbf{\Gamma}(\{p\}, \mu) = \mathbf{\Gamma}_{\text{dip}}(\{p\}, \mu) + \mathbf{\Delta}_3(\{p\}, \mu). \quad (25)$$

The former is due to the pairwise exchange of color charge be-

tween external legs and reads

$$\begin{aligned} \mathbf{\Gamma}_{\text{dip}}(\{p\}, \mu) &= \sum_{1 \leq i < j \leq n} \mathbf{T}_i^a \mathbf{T}_j^a \gamma^K(\alpha_s) \log \left(- \frac{\mu^2}{s_{ij} + i\eta} \right) \\ &+ \sum_{i=1}^n \gamma^i(\alpha_s), \end{aligned} \quad (26)$$

where the γ^K is the cusp anomalous dimension and γ^i is the anomalous dimension of parton i .

The quadrupole contribution $\mathbf{\Delta}_3$ in eq. (25) accounts for the exchange of color charge among three or four soft gluons emitted from (a subset of) the partonic legs. Unlike in three-loop four-parton scattering [7–9, 34] where this term was observed in N=4 SYM and QCD amplitudes for the first time, soft gluon emissions from four external partons are impossible here and thus the quadrupole term consists only of the entirely kinematics-independent term [1]

$$\mathbf{\Delta}_3^{(3),ijk} = -f_{abe} f_{cde} \left[16C \sum_{i=1}^3 \sum_{\substack{1 \leq j < k \leq 3 \\ j,k \neq i}} \{ \mathbf{T}_i^a, \mathbf{T}_i^d \} \mathbf{T}_j^b \mathbf{T}_k^c \right], \quad (27)$$

with $C = \zeta_5 + 2\zeta_2\zeta_3$ a constant. However, this term only enters the color layers that are suppressed by at least N^{-2} relative to the leading color contributions considered here.

In summary, given the l -loop renormalized helicity amplitudes $\mathbf{\Phi}^{(l)}$, one can remove the IR singularities with

$$\begin{aligned} \mathbf{\Phi}_{\text{finite}}^{(0)} &= \mathbf{\Phi}^{(0)}, \\ \mathbf{\Phi}_{\text{finite}}^{(1)} &= \mathbf{\Phi}^{(1)} - \mathbf{I}^{(1)} \mathbf{\Phi}^{(0)}, \\ \mathbf{\Phi}_{\text{finite}}^{(2)} &= \mathbf{\Phi}^{(2)} - \mathbf{I}^{(2)} \mathbf{\Phi}^{(0)} - \mathbf{I}^{(1)} \mathbf{\Phi}^{(1)}, \\ \mathbf{\Phi}_{\text{finite}}^{(3)} &= \mathbf{\Phi}^{(3)} - \mathbf{I}^{(3)} \mathbf{\Phi}^{(0)} - \mathbf{I}^{(2)} \mathbf{\Phi}^{(1)} - \mathbf{I}^{(1)} \mathbf{\Phi}^{(2)}. \end{aligned} \quad (28)$$

The subtraction operators in (28) can be expressed as

$$\begin{aligned} \mathbf{I}^{(1)} &= \mathcal{Z}^{(1)}, \\ \mathbf{I}^{(2)} &= \mathcal{Z}^{(2)} - (\mathcal{Z}^{(1)})^2, \\ \mathbf{I}^{(3)} &= \mathcal{Z}^{(3)} - 2\mathcal{Z}^{(2)}\mathcal{Z}^{(1)} + (\mathcal{Z}^{(1)})^3. \end{aligned} \quad (29)$$

After performing the color algebra in (28), we recover the simple factorizing structure (23) for the finite parts of the helicity amplitude. Consequently, (28) also holds for the amplitude coefficients Ω .

As explained in detail in [21], the explicit form of the operators \mathcal{Z}_i in terms of the universal constants in the perturbative expansion for γ^K , γ^q and γ^g is implied by the dipole formula (26) and the new term $\mathbf{\Delta}_3^{(3)}$. A summary of the relevant expressions for UV renormalization and IR subtraction is given in the supplemental material.

4. Results

In view of future phenomenological applications of the three-loop $Vq\bar{q}g$ amplitudes to LHC physics, we perform the analytic

	$V \rightarrow gq\bar{q}$	$q\bar{q} \rightarrow Vg$	$qg \rightarrow Vq$	$\bar{q}g \rightarrow V\bar{q}$
	$y = z = 1/3$	$u = 1/7, v = 3/5$		
α_1	$0.59426734 + 0.03099861i$	$-0.49538117 + 0.65353908i$	$-0.22197101 - 0.03494388i$	$-0.22197101 - 0.03494388i$
α_2	$1.7192645 - 8.7893957i$	$2.0901940 + 8.1000376i$	$-1.6429881 + 0.5830600i$	$-1.6429881 + 0.5830600i$
α_3	$1.2128210 + 5.9479256i$	$-6.0948209 - 9.3383011i$	$0.94229209 - 0.78134227i$	$0.94229209 - 0.78134227i$
γ_1	$-0.59426734 - 0.03099861i$	$0.46544666 - 1.05443048i$	$-0.05750758 + 0.15110700i$	$-0.05750758 + 0.15110700i$
γ_2	$-1.7192645 + 8.7893957i$	$-1.0680269 - 9.5317293i$	$0.24066096 - 0.32042746i$	$0.24066096 - 0.32042746i$
γ_3	$1.2128210 + 5.9479256i$	$-5.2865869 - 7.5133951i$	$0.18231060 + 0.07136413i$	$0.18231060 + 0.07136413i$

Table 1: Numerical values for the finite remainders of the helicity coefficients at a phase-space point in each channel to 8 significant figures, setting $q^2 = 1$, $N = 3$ and $N_f = 5$. All values are to be multiplied by 10^4 .

continuation of the V decay amplitudes to the kinematic regions where the electroweak boson is produced in addition to a jet from the scattering of two partons: $qg \rightarrow Vq$, $\bar{q}g \rightarrow V\bar{q}$ and $q\bar{q} \rightarrow Vg$.

The general strategy for performing the analytic continuation of the MPLs appearing in $2 \rightarrow 2$ scattering involving four-point functions with one off-shell leg and massless propagators was outlined in detail in [27] and adapted for the case of $Vq\bar{q}g$ in [22]. In summary, we can access all the production helicity amplitudes by combinations of kinematic crossings of the external momenta, parity flips and the analytic continuation of MPLs to the region denoted as (3a) in [27] via the substitution

$$y = 1/v, \quad z = -u/v. \quad (30)$$

The finite remainders of the independent helicity amplitudes in the decay and production regions constitute the main result of this work and are linked in electronic format to the `ARXIV` submission of this letter.

The provided results are compact and can easily be evaluated numerically for phenomenological studies. To demonstrate this, in table 1 we present values for the helicity coefficients at the symmetric phase space point $y = z = 1 - y - z = 1/3$ in decay kinematics (where the coefficients α and γ take the same absolute value and where all imaginary parts are generated from the expansion of the overall factors $(-q^2)^{-\epsilon}$) and at a selected point in each of the production regimes. The values were obtained using `GiNAC` [51] as implemented in `POLYLOGTOOLS` [16].

We verified that in all helicity configurations, the symbol of the leading colour $Vgq\bar{q}$ amplitude satisfies the conjectured non-adjacency conditions [15]. It was found in [33] that in the tennis-court topology, a single master integral with 8 propagators and its crossing have a symbol with $1-z$ and $1-x$ appearing next to each other. This violation propagates to several higher topologies during integration and the cancellation of the violating symbol in the amplitude is therefore non-trivial.

5. Conclusions

In this letter, we presented the first calculation of a planar three-loop four-point amplitude in QCD with an external mass. This calculation opens the door to a wealth of three-loop amplitudes, indispensable to precision phenomenology at hadron colliders: V +jet production at the LHC or three-jet production

at lepton colliders, as well as the production of a Higgs boson with a jet. As the present calculation stretches current methods to their computational limit, these tasks will require a concerted effort on the completion of the non-planar integrals, the study of the special functions which appear within, as well as new ideas for IBP reduction and improvements in computer algebra for handling large intermediate expressions. In turn, the availability of three-loop amplitudes will enable precision phenomenology at N³LO in QCD, which is necessary to reach the percent-level goal ahead of the High-Luminosity run at the LHC.

Acknowledgments

This work was supported in part by the Excellence Cluster ORIGINS funded by the Deutsche Forschungsgemeinschaft (DFG, German Research Foundation) under Germany's Excellence Strategy – EXC-2094-390783311, by the Swiss National Science Foundation (SNF) under contract 200020-204200, and by the European Research Council (ERC) under the European Union's research and innovation programme grant agreements 949279 (ERC Starting Grant HighPHun) and 101019620 (ERC Advanced Grant TOPUP).

Appendix A. UV renormalization

In this supplemental material, we collect key formulas relevant to the calculation of the three-loop helicity amplitude coefficients and to their renormalization and infrared subtraction. The first three β -function coefficients are

$$\beta_0 = \frac{11C_A}{6} - \frac{2T_R N_f}{3}, \quad (\text{A.1})$$

$$\beta_1 = \frac{17C_A^2}{6} - \frac{5C_A T_R N_f}{3} - C_F T_R N_f, \quad (\text{A.2})$$

$$\beta_2 = -\frac{205}{72} C_A C_F N_f T_R - \frac{1415}{216} C_A^2 N_f T_R + \frac{79}{108} C_A N_f^2 T_R^2 + \frac{2857C_A^3}{432} + \frac{11}{18} C_F N_f^2 T_R^2 + \frac{1}{4} C_F^2 N_f T_R, \quad (\text{A.3})$$

with the QCD colour factors

$$C_A = N, \quad C_F = \frac{N^2 - 1}{2N}, \quad T_R = \frac{1}{2}. \quad (\text{A.4})$$

Appendix B. IR subtraction

We define the expansions

$$\Gamma_{\text{dip}} = \sum_{l=0}^{\infty} \Gamma_l \left(\frac{\alpha_s}{2\pi} \right)^{l+1}, \quad \Gamma' = \frac{\partial \Gamma_{\text{dip}}}{\partial \log(\mu)} = \sum_{l=0}^{\infty} \Gamma'_l \left(\frac{\alpha_s}{2\pi} \right)^{l+1}. \quad (\text{B.1})$$

Both of the operators diagonalize in colour space for a process with three partons so we can drop the boldface notation. Substituting into (24), we obtain

$$\mathcal{Z}^{(1)} = \frac{\Gamma'_0}{4\epsilon^2} + \frac{\Gamma_0}{2\epsilon} \quad (\text{B.2})$$

$$\mathcal{Z}^{(2)} = \frac{\Gamma_0^2}{32\epsilon^4} + \frac{\Gamma'_0}{8\epsilon^3} \left(\Gamma_0 - \frac{3\beta_0}{2} \right) + \frac{1}{4\epsilon^2} \left(-\beta_0 \Gamma_0 + \frac{\Gamma_0^2}{2} + \frac{\Gamma_1}{4} \right) + \frac{\Gamma_1}{4\epsilon} \quad (\text{B.3})$$

$$\begin{aligned} \mathcal{Z}^{(3)} = & + \frac{\Gamma_0^3}{384\epsilon^6} + \frac{\Gamma_0^2}{64\epsilon^5} (\Gamma_0 - 3\beta_0) + \frac{\Gamma'_0}{9\epsilon^4} \left(-\frac{5}{4}\beta_0 \Gamma_0 + \frac{11}{9}\beta_0^2 + \frac{1}{4}\Gamma_0^2 + \frac{\Gamma_1}{8} \right) \\ & + \frac{1}{\epsilon^3} \left(\frac{1}{54}\Gamma_0' (10C_A N_f T_R - 17C_A^2 + 6C_F N_f T_R) + \Gamma_0 \left(\frac{\beta_0^2}{6} + \frac{\Gamma_1}{32} \right) - \frac{1}{8}\beta_0 \Gamma_0^2 - \frac{5\beta_0 \Gamma_1'}{72} + \frac{\Gamma_1 \Gamma_0'}{16} + \frac{\Gamma_0^3}{48} \right) \\ & + \frac{1}{\epsilon^2} \left(\Gamma_0 \left(\frac{1}{36} (10C_A N_f T_R - 17C_A^2 + 6C_F N_f T_R) + \frac{\Gamma_1}{8} \right) - \frac{\beta_0 \Gamma_1}{6} + \frac{\Gamma_2'}{36} \right) + \frac{\Gamma_2 + \Delta_3^{(3)}}{6\epsilon}. \end{aligned} \quad (\text{B.4})$$

Defining a perturbative expansion for the anomalous dimensions with $i = K, q, \bar{q}, g$,

$$\gamma^i = \sum_{l=0}^{\infty} \gamma_l^i \left(\frac{\alpha_s}{2\pi} \right)^{l+1}, \quad (\text{B.5})$$

we can use the dipole formula to write for the $gq\bar{q}$ system

$$\Gamma_l = -C_F L_{12} \gamma_l^K - \frac{C_A}{2} (-L_{12} + L_{23} + L_{13}) \gamma_l^K + 2\gamma_l^q + \gamma_l^g, \quad (\text{B.6})$$

$$\Gamma'_l = -\gamma^K(\alpha_s)(2C_F + C_A), \quad (\text{B.7})$$

with

$$L_{ij} = \log \left(-\frac{\mu^2}{s_{ij} + i\eta} \right). \quad (\text{B.8})$$

For convenience, we also reproduce the first three coefficients for the cusp anomalous dimension

$$\gamma_0^K = 2 \quad (\text{B.9})$$

$$\gamma_1^K = \left(\frac{67}{9} - \frac{\pi^2}{3} \right) C_A - \frac{10N_f}{9} \quad (\text{B.10})$$

$$\gamma_2^K = \left(-\frac{14\zeta_3}{3} + \frac{10\pi^2}{27} - \frac{209}{54} \right) C_A N_f + \left(\frac{11\zeta_3}{3} + \frac{11\pi^4}{90} - \frac{67\pi^2}{27} + \frac{245}{12} \right) C_A^2 + \left(4\zeta_3 - \frac{55}{12} \right) C_F N_f - \frac{2N_f^2}{27}, \quad (\text{B.11})$$

the quark anomalous dimension

$$\gamma_0^q = -\frac{3C_F}{2} \quad (\text{B.12})$$

$$\gamma_1^q = \left(\frac{13\zeta_3}{2} - \frac{11\pi^2}{24} - \frac{961}{216} \right) C_A C_F + \left(\frac{65}{108} + \frac{\pi^2}{12} \right) C_F N_f + \left(-6\zeta_3 + \frac{\pi^2}{2} - \frac{3}{8} \right) C_F^2 \quad (\text{B.13})$$

$$\begin{aligned} \gamma_2^q = & \left(-\frac{241\zeta_3}{54} + \frac{11\pi^4}{360} + \frac{1297\pi^2}{1944} - \frac{8659}{5832} \right) C_A C_F N_f + \left(-\frac{1}{3}\pi^2\zeta_3 - \frac{211\zeta_3}{6} - 15\zeta_5 + \frac{247\pi^4}{1080} + \frac{205\pi^2}{72} - \frac{151}{32} \right) C_A C_F^2 \\ & + \left(-\frac{11}{18}\pi^2\zeta_3 + \frac{1763\zeta_3}{36} - 17\zeta_5 - \frac{83\pi^4}{720} - \frac{7163\pi^2}{3888} - \frac{139345}{23328} \right) C_A^2 C_F + \left(\frac{32\zeta_3}{9} - \frac{7\pi^4}{108} - \frac{13\pi^2}{72} + \frac{2953}{432} \right) C_F^2 N_f \\ & + \left(-\frac{\zeta_3}{27} - \frac{5\pi^2}{108} + \frac{2417}{5832} \right) C_F N_f^2 + \left(\frac{2\pi^2\zeta_3}{3} - \frac{17\zeta_3}{2} + 30\zeta_5 - \frac{\pi^4}{5} - \frac{3\pi^2}{8} - \frac{29}{16} \right) C_F^3, \end{aligned} \quad (\text{B.14})$$

and the gluon anomalous dimension

$$\gamma_0^g = -\beta_0 \quad (\text{B.15})$$

$$\gamma_1^g = \left(\frac{32}{27} - \frac{\pi^2}{36} \right) C_A N_f + \left(\frac{\zeta_3}{2} + \frac{11\pi^2}{72} - \frac{173}{27} \right) C_A^2 + \frac{C_F N_f}{2} \quad (\text{B.16})$$

$$\begin{aligned} \gamma_2^g = & \left(-\frac{19\zeta_3}{9} - \frac{\pi^4}{90} - \frac{\pi^2}{24} + \frac{1217}{216} \right) C_A C_F N_f + \left(-\frac{7\zeta_3}{27} + \frac{5\pi^2}{324} - \frac{269}{11664} \right) C_A N_f^2 - \frac{11}{72} C_F N_f^2 - \frac{1}{8} C_F^2 N_f \\ & + \left(\frac{89\zeta_3}{54} + \frac{41\pi^4}{1080} - \frac{599\pi^2}{1944} + \frac{30715}{11664} \right) C_A^2 N_f + \left(-\frac{5}{18}\pi^2\zeta_3 + \frac{61\zeta_3}{12} - 2\zeta_5 - \frac{319\pi^4}{2160} + \frac{6109\pi^2}{3888} - \frac{48593}{2916} \right) C_A^3. \end{aligned} \quad (\text{B.17})$$

Appendix C. Projectors onto helicity amplitude coefficients

With the common denominator $\mathcal{D} = 2(d-3)y^3z^2(1-y-z)^2$ and the tensor basis defined as in ref. [22],

$$\begin{aligned} \mathcal{P}_{\alpha_1} = & \frac{1}{\mathcal{D}} \left[-d(1-y)^2z T_1^\dagger + z(-2y(-1+y+2z) + d(-1+y+z+yz)) T_2^\dagger - (1-y)yz(1-y-z) T_3^\dagger \right. \\ & \left. + (1-y)^2yz T_4^\dagger - yz(-1+y+z+yz) T_5^\dagger + (1-y)yz^2 T_6^\dagger \right], \end{aligned} \quad (\text{C.1})$$

$$\begin{aligned} \mathcal{P}_{\alpha_2} = & \frac{1}{\mathcal{D}} \left[-z(-(d-4)y^2 + (d-4)y(1-z) + dz) T_1^\dagger + z(2y^2 - d(1-z)z + y(-4+d+(2+d)z)) T_2^\dagger \right. \\ & \left. - yz(1-y-z)(y+z) T_3^\dagger - yz(z+y(1-y-z)) T_4^\dagger - yz(y-(1-y)z+z^2) T_5^\dagger + yz^2(y+z) T_6^\dagger \right], \end{aligned} \quad (\text{C.2})$$

$$\mathcal{P}_{\alpha_3} = \frac{1}{\mathcal{D}} \left[+4(1-y)yz(1-y-z) T_1^\dagger + 4yz(1-y-z)^2 T_2^\dagger + 2y^2z(1-y-z)^2 T_3^\dagger - 2y^2z^2(1-y-z) T_6^\dagger \right], \quad (\text{C.3})$$

$$\begin{aligned} \mathcal{P}_{\gamma_1} = & \frac{1}{\mathcal{D}} \left[+(d-4)y(-1+y+z+yz) T_1^\dagger + y(1-z)(-4+d+2y+4z-dz) T_2^\dagger - y^2(1-z)(1-y-z) T_3^\dagger \right. \\ & \left. - y^2(-1+y+z+yz) T_4^\dagger + y^2(1-z)^2 T_5^\dagger - y^2(1-z)z T_6^\dagger \right], \end{aligned} \quad (\text{C.4})$$

$$\begin{aligned} \mathcal{P}_{\gamma_2} = & \frac{1}{\mathcal{D}} \left[+(d-4)y(z-y(1-y-z)) T_1^\dagger + y(2y^2 + (d-4)(1-z)z + y(-4+d-(d-2)z)) T_2^\dagger \right. \\ & \left. - y^2(1-y-z)(y+z) T_3^\dagger - y^2(z-y(1-y-z)) T_4^\dagger + y^2(y-(1-y)z+z^2) T_5^\dagger - y^2z(y+z) T_6^\dagger \right], \end{aligned} \quad (\text{C.5})$$

$$\mathcal{P}_{\gamma_3} = \frac{1}{\mathcal{D}} \left[+4y^2z(1-y-z) T_2^\dagger - 2y^2z(1-y-z)^2 T_3^\dagger - 2y^2z^2(1-y-z) T_6^\dagger \right]. \quad (\text{C.6})$$

References

- [1] Almelid, O., Duhr, C., Gardi, E., 2016. Three-loop corrections to the soft anomalous dimension in multileg scattering. *Phys. Rev. Lett.* 117, 172002. doi:[10.1103/PhysRevLett.117.172002](https://doi.org/10.1103/PhysRevLett.117.172002), [arXiv:1507.00047](https://arxiv.org/abs/1507.00047).
- [2] Arkani-Hamed, N., Bourjaily, J.L., Cachazo, F., Trnka, J., 2012. Local Integrals for Planar Scattering Amplitudes. *JHEP* 06, 125. doi:[10.1007/JHEP06\(2012\)125](https://doi.org/10.1007/JHEP06(2012)125), [arXiv:1012.6032](https://arxiv.org/abs/1012.6032).
- [3] Becher, T., Neubert, M., 2009. On the Structure of Infrared Singularities of Gauge-Theory Amplitudes. *JHEP* 06, 081. doi:[10.1088/1126-6708/2009/06/081](https://doi.org/10.1088/1126-6708/2009/06/081), [10.1007/JHEP11\(2013\)024](https://doi.org/10.1007/JHEP11(2013)024), [arXiv:0903.1126](https://arxiv.org/abs/0903.1126).
- [4] Boughezal, R., Focke, C., Liu, X., Petriello, F., 2015. W -boson production in association with a jet at next-to-next-to-leading order in perturbative QCD. *Phys. Rev. Lett.* 115, 062002. doi:[10.1103/PhysRevLett.115.062002](https://doi.org/10.1103/PhysRevLett.115.062002), [arXiv:1504.02131](https://arxiv.org/abs/1504.02131).
- [5] Canko, D.D., Syrrakos, N., 2022. Planar three-loop master integrals for $2 \rightarrow 2$ processes with one external massive particle. *JHEP* 04, 134. doi:[10.1007/JHEP04\(2022\)134](https://doi.org/10.1007/JHEP04(2022)134), [arXiv:2112.14275](https://arxiv.org/abs/2112.14275).
- [6] Canko, D.D., Syrrakos, N., 2023. Three-loop master integrals for H+jet production at N³LO: Towards the non-planar topologies, in: 16th International Symposium on Radiative Corrections: Applications of Quantum Field Theory to Phenomenology. [arXiv:2307.08432](https://arxiv.org/abs/2307.08432).
- [7] Caola, F., Chakraborty, A., Gambuti, G., von Manteuffel, A., Tancredi, L., 2021. Three-loop helicity amplitudes for four-quark scattering in massless QCD. *JHEP* 10, 206. doi:[10.1007/JHEP10\(2021\)206](https://doi.org/10.1007/JHEP10(2021)206), [arXiv:2108.00055](https://arxiv.org/abs/2108.00055).
- [8] Caola, F., Chakraborty, A., Gambuti, G., von Manteuffel, A., Tancredi, L., 2022a. Three-Loop Gluon Scattering in QCD and the Gluon Regge Trajectory. *Phys. Rev. Lett.* 128, 212001. doi:[10.1103/PhysRevLett.128.212001](https://doi.org/10.1103/PhysRevLett.128.212001), [arXiv:2112.11097](https://arxiv.org/abs/2112.11097).
- [9] Caola, F., Chakraborty, A., Gambuti, G., von Manteuffel, A., Tancredi, L., 2022b. Three-loop helicity amplitudes for quark-gluon scattering in QCD. *JHEP* 12, 082. doi:[10.1007/JHEP12\(2022\)082](https://doi.org/10.1007/JHEP12(2022)082), [arXiv:2207.03503](https://arxiv.org/abs/2207.03503).
- [10] Catani, S., 1998. The Singular behavior of QCD amplitudes at two loop order. *Phys. Lett. B* 427, 161–171. doi:[10.1016/S0370-2693\(98\)00332-3](https://doi.org/10.1016/S0370-2693(98)00332-3), [arXiv:hep-ph/9802439](https://arxiv.org/abs/hep-ph/9802439).
- [11] Catani, S., Seymour, M.H., 1996. The Dipole formalism for the calculation of QCD jet cross-sections at next-to-leading order. *Phys. Lett. B* 378, 287–301. doi:[10.1016/0370-2693\(96\)00425-X](https://doi.org/10.1016/0370-2693(96)00425-X), [arXiv:hep-ph/9602277](https://arxiv.org/abs/hep-ph/9602277).
- [12] Chetyrkin, K., Tkachov, F., 1981. Integration by Parts: The Algorithm to Calculate beta Functions in 4 Loops. *Nucl. Phys. B* 192, 159–204. doi:[10.1016/0550-3213\(81\)90199-1](https://doi.org/10.1016/0550-3213(81)90199-1).
- [13] Di Vita, S., Mastrolia, P., Schubert, U., Yundin, V., 2014. Three-loop master integrals for ladder-box diagrams with one massive leg. *JHEP* 09, 148. doi:[10.1007/JHEP09\(2014\)148](https://doi.org/10.1007/JHEP09(2014)148), [arXiv:1408.3107](https://arxiv.org/abs/1408.3107).
- [14] Dixon, L.J., Gardi, E., Magnea, L., 2010. On soft singularities at three loops and beyond. *JHEP* 02, 081. doi:[10.1007/JHEP02\(2010\)081](https://doi.org/10.1007/JHEP02(2010)081), [arXiv:0910.3653](https://arxiv.org/abs/0910.3653).
- [15] Dixon, L.J., McLeod, A.J., Wilhelm, M., 2021. A Three-Point Form Factor Through Five Loops. *JHEP* 04, 147. doi:[10.1007/JHEP04\(2021\)147](https://doi.org/10.1007/JHEP04(2021)147), [arXiv:2012.12286](https://arxiv.org/abs/2012.12286).
- [16] Duhr, C., Dulat, F., 2019. PolyLogTools — polylogs for the masses. *JHEP* 08, 135. doi:[10.1007/JHEP08\(2019\)135](https://doi.org/10.1007/JHEP08(2019)135), [arXiv:1904.07279](https://arxiv.org/abs/1904.07279).
- [17] Ellis, J.R., Gaillard, M.K., Ross, G.G., 1976. Search for Gluons in e^+e^- Annihilation. *Nucl. Phys. B* 111, 253. doi:[10.1016/0550-3213\(77\)90253-X](https://doi.org/10.1016/0550-3213(77)90253-X) [Erratum: *Nucl. Phys. B* 130, 516 (1977)].
- [18] Ellis, R.K., Ross, D.A., Terrano, A.E., 1981. The Perturbative Calculation of Jet Structure in e^+e^- Annihilation. *Nucl. Phys. B* 178, 421–456. doi:[10.1016/0550-3213\(81\)90165-6](https://doi.org/10.1016/0550-3213(81)90165-6).
- [19] Gardi, E., Magnea, L., 2009. Factorization constraints for soft anomalous dimensions in QCD scattering amplitudes. *JHEP* 03, 079. doi:[10.1088/1126-6708/2009/03/079](https://doi.org/10.1088/1126-6708/2009/03/079), [arXiv:0901.1091](https://arxiv.org/abs/0901.1091).
- [20] Garland, L.W., Gehrmann, T., Glover, E.W.N., Koukoutsakis, A., Remiddi, E., 2002. Two loop QCD helicity amplitudes for $e^+e^- \rightarrow 3$ jets. *Nucl. Phys. B* 642, 227–262. doi:[10.1016/S0550-3213\(02\)00627-2](https://doi.org/10.1016/S0550-3213(02)00627-2), [arXiv:hep-ph/0206067](https://arxiv.org/abs/hep-ph/0206067).
- [21] Gehrmann, T., Jakubčík, P., Mella, C.C., Syrrakos, N., Tancredi, L., 2023a. Two-loop helicity amplitudes for H +jet production to higher orders in the dimensional regulator. *JHEP* 04, 016. doi:[10.1007/JHEP04\(2023\)016](https://doi.org/10.1007/JHEP04(2023)016), [arXiv:2301.10849](https://arxiv.org/abs/2301.10849).
- [22] Gehrmann, T., Jakubčík, P., Mella, C.C., Syrrakos, N., Tancredi, L., 2023b. Two-loop helicity amplitudes for V +jet production including axial vector couplings to higher orders in ϵ [arXiv:2306.10170](https://arxiv.org/abs/2306.10170).
- [23] Gehrmann, T., Peraro, T., Tancredi, L., 2023c. Two-loop QCD corrections to the $V \rightarrow q\bar{q}g$ helicity amplitudes with axial-vector couplings. *JHEP* 02, 041. doi:[10.1007/JHEP02\(2023\)041](https://doi.org/10.1007/JHEP02(2023)041), [arXiv:2211.13596](https://arxiv.org/abs/2211.13596).
- [24] Gehrmann, T., Remiddi, E., 2000. Differential equations for two loop four point functions. *Nucl. Phys. B* 580, 485–518. doi:[10.1016/S0550-3213\(00\)00223-6](https://doi.org/10.1016/S0550-3213(00)00223-6), [arXiv:hep-ph/9912329](https://arxiv.org/abs/hep-ph/9912329).
- [25] Gehrmann, T., Remiddi, E., 2001a. Two loop master integrals for $\gamma^* \rightarrow 3$ jets: The Nonplanar topologies. *Nucl. Phys. B* 601, 287–317. doi:[10.1016/S0550-3213\(01\)00074-8](https://doi.org/10.1016/S0550-3213(01)00074-8), [arXiv:hep-ph/0101124](https://arxiv.org/abs/hep-ph/0101124).
- [26] Gehrmann, T., Remiddi, E., 2001b. Two loop master integrals for $\gamma^* \rightarrow 3$ jets: The Planar topologies. *Nucl. Phys. B* 601, 248–286. doi:[10.1016/S0550-3213\(01\)00057-8](https://doi.org/10.1016/S0550-3213(01)00057-8), [arXiv:hep-ph/0008287](https://arxiv.org/abs/hep-ph/0008287).
- [27] Gehrmann, T., Remiddi, E., 2002. Analytic continuation of massless two loop four point functions. *Nucl. Phys. B* 640, 379–411. doi:[10.1016/S0550-3213\(02\)00569-2](https://doi.org/10.1016/S0550-3213(02)00569-2), [arXiv:hep-ph/0207020](https://arxiv.org/abs/hep-ph/0207020).
- [28] Gehrmann-De Ridder, A., Gehrmann, T., Glover, E.W.N., Heinrich, G., 2007. NNLO corrections to event shapes in e^+e^- annihilation. *JHEP* 12, 094. doi:[10.1088/1126-6708/2007/12/094](https://doi.org/10.1088/1126-6708/2007/12/094), [arXiv:0711.4711](https://arxiv.org/abs/0711.4711).
- [29] Gehrmann-De Ridder, A., Gehrmann, T., Glover, E.W.N., Heinrich, G., 2014. EERAD3: Event shapes and jet rates in electron-positron annihilation at order α_s^3 . *Comput. Phys. Commun.* 185, 3331. doi:[10.1016/j.cpc.2014.07.024](https://doi.org/10.1016/j.cpc.2014.07.024), [arXiv:1402.4140](https://arxiv.org/abs/1402.4140).
- [30] Gehrmann-De Ridder, A., Gehrmann, T., Glover, E.W.N., Huss, A., Morgan, T.A., 2016. Precise QCD predictions for the production of a Z boson in association with a hadronic jet. *Phys. Rev. Lett.* 117, 022001. doi:[10.1103/PhysRevLett.117.022001](https://doi.org/10.1103/PhysRevLett.117.022001), [arXiv:1507.02850](https://arxiv.org/abs/1507.02850).
- [31] Giele, W.T., Glover, E.W.N., 1992. Higher order corrections to jet cross-sections in e^+e^- annihilation. *Phys. Rev. D* 46, 1980–2010. doi:[10.1103/PhysRevD.46.1980](https://doi.org/10.1103/PhysRevD.46.1980).
- [32] Goncharov, A.B., 1998. Multiple polylogarithms, cyclotomy and modular complexes. *Math. Res. Lett.* 5, 497–516. doi:[10.4310/MRL.1998.v5.n4.a7](https://doi.org/10.4310/MRL.1998.v5.n4.a7), [arXiv:1105.2076](https://arxiv.org/abs/1105.2076).
- [33] Henn, J.M., Lim, J., Torres Bobadilla, W.J., 2023. First look at the evaluation of three-loop non-planar Feynman diagrams for Higgs plus jet production [arXiv:2302.12776](https://arxiv.org/abs/2302.12776).
- [34] Henn, J.M., Mistlberger, B., 2016. Four-Gluon Scattering at Three Loops, Infrared Structure, and the Regge Limit. *Phys. Rev. Lett.* 117, 171601. doi:[10.1103/PhysRevLett.117.171601](https://doi.org/10.1103/PhysRevLett.117.171601), [arXiv:1608.00850](https://arxiv.org/abs/1608.00850).
- [35] Henn, J.M., Smirnov, A.V., Smirnov, V.A., 2014. Evaluating single-scale and/or non-planar diagrams by differential equations. *JHEP* 1403, 088. doi:[10.1007/JHEP03\(2014\)088](https://doi.org/10.1007/JHEP03(2014)088), [arXiv:1312.2588](https://arxiv.org/abs/1312.2588).
- [36] 't Hooft, G., Veltman, M.J.G., 1972. Regularization and Renormalization of Gauge Fields. *Nucl. Phys. B* 44, 189–213. doi:[10.1016/0550-3213\(72\)90279-9](https://doi.org/10.1016/0550-3213(72)90279-9).
- [37] Klappert, J., Lange, F., Maierhöfer, P., Usovitsch, J., 2021. Integral reduction with Kira 2.0 and finite field methods. *Comput. Phys. Commun.* 266, 108024. doi:[10.1016/j.cpc.2021.108024](https://doi.org/10.1016/j.cpc.2021.108024), [arXiv:2008.06494](https://arxiv.org/abs/2008.06494).
- [38] Kotikov, A., 1991. Differential equations method: New technique for massive Feynman diagrams calculation. *Phys. Lett. B* 254, 158–164. doi:[10.1016/0370-2693\(91\)90413-K](https://doi.org/10.1016/0370-2693(91)90413-K).
- [39] Kunszt, Z., Nason, P., Marchesini, G., Webber, B.R., 1989. QCD at LEP, in: LEP Physics Workshop.
- [40] Laporta, S., 2000. High precision calculation of multiloop Feynman integrals by difference equations. *Int.J.Mod.Phys. A* 15, 5087–5159. doi:[10.1016/S0217-751X\(00\)00215-7](https://doi.org/10.1016/S0217-751X(00)00215-7), [arXiv:hep-ph/0102033](https://arxiv.org/abs/hep-ph/0102033).
- [41] Maierhöfer, P., Usovitsch, J., Uwer, P., 2018. Kira—A Feynman integral reduction program. *Comput. Phys. Commun.* 230, 99–112. doi:[10.1016/j.cpc.2018.04.012](https://doi.org/10.1016/j.cpc.2018.04.012), [arXiv:1705.05610](https://arxiv.org/abs/1705.05610).
- [42] von Manteuffel, A., Schabinger, R.M., 2015. A novel approach to integration by parts reduction. *Phys. Lett. B* 744, 101–104. doi:[10.1016/j.physletb.2015.03.029](https://doi.org/10.1016/j.physletb.2015.03.029), [arXiv:1406.4513](https://arxiv.org/abs/1406.4513).
- [43] Neumann, T., Campbell, J., 2023. Fiducial Drell-Yan production at the LHC improved by transverse-momentum resummation at N⁴LLp+N³LO. *Phys. Rev. D* 107, L011506. doi:[10.1103/PhysRevD.107.L011506](https://doi.org/10.1103/PhysRevD.107.L011506), [arXiv:2207.07056](https://arxiv.org/abs/2207.07056).
- [44] Nogueira, P., 1993. Automatic Feynman graph generation. *J. Comput.*

- Phys. 105, 279–289. doi:[10.1006/jcph.1993.1074](https://doi.org/10.1006/jcph.1993.1074).
- [45] Peraro, T., 2019. FiniteFlow: multivariate functional reconstruction using finite fields and dataflow graphs. JHEP 07, 031. doi:[10.1007/JHEP07\(2019\)031](https://doi.org/10.1007/JHEP07(2019)031), [arXiv:1905.08019](https://arxiv.org/abs/1905.08019).
- [46] Peraro, T., Tancredi, L., 2019. Physical projectors for multi-leg helicity amplitudes. JHEP 07, 114. doi:[10.1007/JHEP07\(2019\)114](https://doi.org/10.1007/JHEP07(2019)114), [arXiv:1906.03298](https://arxiv.org/abs/1906.03298).
- [47] Peraro, T., Tancredi, L., 2021. Tensor decomposition for bosonic and fermionic scattering amplitudes. Phys. Rev. D 103, 054042. doi:[10.1103/PhysRevD.103.054042](https://doi.org/10.1103/PhysRevD.103.054042), [arXiv:2012.00820](https://arxiv.org/abs/2012.00820).
- [48] Remiddi, E., Vermaseren, J., 2000. Harmonic polylogarithms. Int.J.Mod.Phys. A15, 725–754. doi:[10.1142/S0217751X00000367](https://doi.org/10.1142/S0217751X00000367), [arXiv:hep-ph/9905237](https://arxiv.org/abs/hep-ph/9905237).
- [49] Tkachov, F., 1981. A Theorem on Analytical Calculability of Four Loop Renormalization Group Functions. Phys. Lett. B100, 65–68. doi:[10.1016/0370-2693\(81\)90288-4](https://doi.org/10.1016/0370-2693(81)90288-4).
- [50] Vermaseren, J.A.M., 2000. New features of FORM [arXiv:math-ph/0010025](https://arxiv.org/abs/math-ph/0010025).
- [51] Vollinga, J., Weinzierl, S., 2005. Numerical evaluation of multiple polylogarithms. Comput.Phys.Commun. 167, 177. doi:[10.1016/j.cpc.2004.12.009](https://doi.org/10.1016/j.cpc.2004.12.009), [arXiv:hep-ph/0410259](https://arxiv.org/abs/hep-ph/0410259).
- [52] Weinzierl, S., 2008. NNLO corrections to 3-jet observables in electron-positron annihilation. Phys. Rev. Lett. 101, 162001. doi:[10.1103/PhysRevLett.101.162001](https://doi.org/10.1103/PhysRevLett.101.162001), [arXiv:0807.3241](https://arxiv.org/abs/0807.3241).